Tuning the Electronic Communication between Iron Carbonyl Fragments Coordinated to Bis-imine Ligands by Variation of the Bridging Unit

Angela Göbel, Guido Leibeling, Manfred Rudolph, and Wolfgang Imhof*

Institut für Anorganische und Analytische Chemie der Friedrich-Schiller-Universität, August-Bebel-Strasse 2, 07743 Jena, Germany

Received October 15, 2002

The reaction of bis-imine ligands, which are synthesized from diamines containing variable bridging units between the amine functions and benzaldehyde, with $Fe_2(CO)_9$ leads to the formation of di- and tetranuclear iron carbonyl complexes. Either one or both imine moieties are coordinated to $Fe_2(CO)_6$ fragments by a C−H activation reaction in ortho-position with respect to the imine group followed by an intramolecular 1,3-hydrogen shift reaction toward the former imine carbon atom. Mössbauer spectroscopy on the tetranuclear complexes suggests that there are two slightly different types of iron atoms, both of which can be described in the oxidation state +1 with $S = 1/2$. Corresponding to this finding, the tetranuclear iron carbonyl compounds may be reduced four times. The cyclic voltammograms show that only the first two reduction steps, which appear at very similar potential, are fully reversible. The difference between these first two reduction potentials may be determined by a complete simulation of the current−voltage characteristic and is found to depend on the nature of the bridging unit between the two iron carbonyl subunits. An effective conjugation between both organometallic moieties correlates with a large difference in the reduction potentials. A similar effect is observed in susceptibility measurements. The smallest magnetic moments are determined for those compounds that show effective communication between the metal centers in the cyclic voltammograms. Obviously the spins being present in the Fe(I) compounds can undergo effective coupling through the bridging unit. Minimizing the interaction between the organometallic subunits leads to the observation of an effective magnetic moment of up to 4.84 μ_B at room temperature, nearly exactly matching the spin-only value of four unpaired electrons.

Introduction

The synthesis of transition metal compounds, in which the metal centers show an electronic communication between each other, has found increasing interest in recent years. The major goal of this research was to assemble subunits containing transition metals by suitable molecular or supramolecular techniques in order to systematically tune their physical properties such as optical or magnetic properties, redox behavior, or their use as catalytically active compounds.[1] A large number of complexes have been synthesized based on metallocene-type transition metal subunits linked by various bridging units because electron transfer processes in such systems are often highly reversible and such compounds exhibit a relatively rigid molecular framework.[1e,2] Promising results toward the synthesis of molecular wires have been achieved by linking organometallic centers by oligoalkynyl bridges.[3]

Quite a few metalloproteins also use the communication between two metal centers in order to achieve a

* Corresponding author. Fax: ++49-3641-948102. E-mail: cwi@rz.uni-jena.de.

(1) (a) Balzani, V.; Scandola, F. *Supramolecular Chemistry*; Ellis Horwood: New York, 1991. (b) Balzani, V.; Moggi, L.; Scandola, F. In *Supramolecular Photochemistry*; Balzani, V., Ed.; Reidel: Dordrecht, 1987. (c) Launay, J.-P., Ed. Molecular Electronics. *New J. Chem.* **1991**, *15*, 97. (d) Astruc, D. *Electron Transfer and Radical Processes in Transition Metal Chemistry*; VCH: New York, 1995. (e) Astruc, D. *Acc. Chem. Res.* **1997**, *30*, 383. (f) Lehn, J.-M. *Supramolecular Chemistry*; VCH: Weinheim, 1995. (g) Dürr, H., Bouas-Laurent, H. H., Eds. *Photochromism: Molecules and Systems*; Elsevier: Amsterdam, 1990. (h) Czarnik, A. W. *Acc. Chem. Res.* **1994**, *27*, 302. (i) James, T. J.; Shinkai, S. *J. Chem. Soc., Chem. Commun.* **1996**, 281. (j) Kahn, O. *Molecular Magnetism*; VCH: New York, 1993. (k) Edmonds, T. E. *Chemical Sensors*; Blackie: Glasgow, 1988. (l) Atwood, J. L.; Holman, K. T.; Steed, J. W. *J. Chem. Soc., Chem. Commun.* **1996**, 1401. (m) Spangenberg, A.; Oberthür, M.; Noss, H.; Tillack, A.; Arndt, P.; Kempe, R. *Angew. Chem., Int. Ed.* **1998**, *37*, 2079. Korybut-Daszkiewicz, B.; Wieckowska, A.; Bilewicz, R.; Domagala, S.; Wozniak, K. *J. Am. Chem. Soc.* **2001**, *123*, 9356.

(2) (a) Barlow, S.; O'Hare, D. *Chem. Rev.* **1997**, *97*, 637. (b) Carmichael, D.; Mathey, F. In Heteroelements et Coordination. *Top. Curr. Chem.* **2002**, *220*, 27. (c) Guo, S. L.; Peters, F.; Fabrizi de Biani, F.; Bats, J. W.; Herdtweck, E.; Zanello, P.; Wagner, M. *Inorg. Chem.* **2001**, *40*, 4928.

(3) (a) Wong, W.-Y.; Choi, K.-H.; Lu, G.-L.; Shi, J.-X.; Lai, P.-Y.; Chan, S.-M.; Lin, Z. *Organometallics* **2001**, *20*, 5446. (b) Kaharu, T.; Matsubara, H.; Takahashi, S. *J. Mater. Chem.* **1991**, *1*, 1. (c) Adroin, N.; Astruc, D. *Bull. Soc. Chim. Fr.* **1995**, *132*, 875. (d) Valério, C.; Fillaut, J. L.; Ruiz, J.; Guittard, J.; Blais, J.-C.; Astruc, D. *J. Am. Chem. Soc.* **1997**, *119*, 2588. (e) Serroni, S.; Denti, G.; Campagna, S.; Juris, A.; Ciano, M.; Balzani, V. *Angew. Chem., Int. Ed. Engl.* **1992**, *31*, 1493. (f) Serroni, S.; Denti, G.; Campagna, S.; Juris, A.; Ciano, M.; Balzani, V. *J. Am. Chem. Soc.* **1992**, *114*, 2944. (g) Bartik, T.; Weng, W.; Ramsden, J. A.; Szafert, S.; Falloon, S. B.; Arif, A. F.; Gladysz, J. A. *J. Am. Chem. Soc.* **1998**, *120*, 11071. (h) Dembinski, R.; Lis, T.; Szafert, S.; Mayne, C. L.; Bartik, T.; Gladysz, J. A. *J. Organomet. Chem.* **1999**, *578*, 229. (i) Meyer, W. E.; Amoroso, A. J.; Horn, C. R.; Jaeger, M.; Gladysz, J. A. *Organometallics* **2001**, *20*, 1115. (j) Peters, T. B.; Zheng, Q.; Stahl, J.; Bohling, J. C.; Arif, A. M.; Hampel, F.; Gladysz, J. A. *J. Organomet. Chem.* **2002**, *641*, 53.

10.1021/om020850i CCC: $25.00
Publication on Web 01/14/2003

Scheme 1

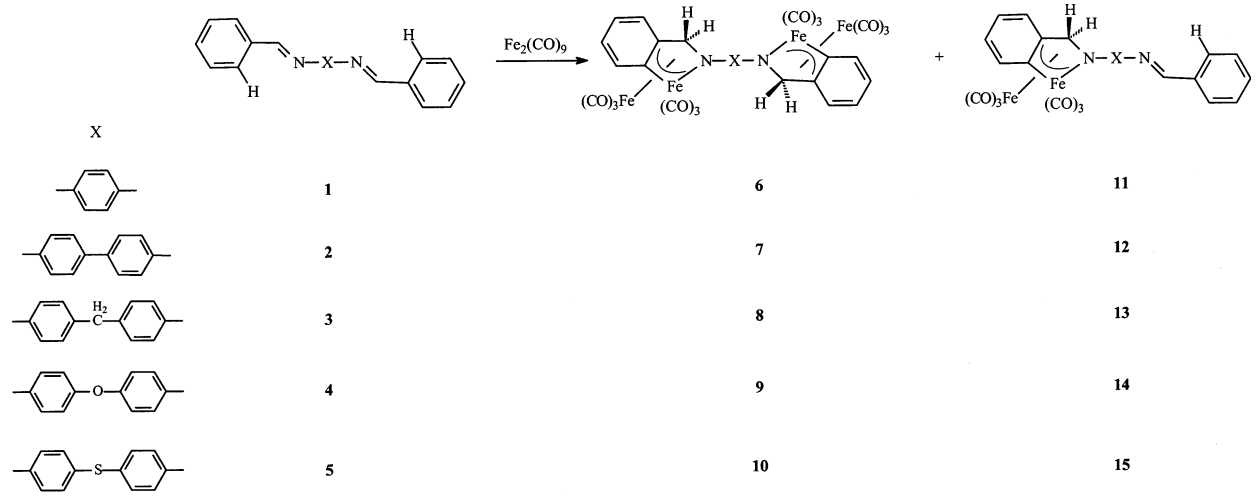

certain reactivity by cooperative effects or to stabilize at least one of the transition metals in a highly reactive oxidation state.[4] A very prominent example of this type of metalloproteins is methanemonooxygenase (MMO), which contains two iron atoms linked by carboxylato bridges from the surrounding protein. The special coordination sphere around the iron dimer allows the activation of dioxygen as well as the subsequent transformation of methane (or even higher alkanes) to methanol by C−H activation steps of the saturated hydrocarbon substrate.[5] The mechanism of this reaction has been investigated both experimentally and theoretically by a number of research groups, because the catalytic functionalization of saturated hydrocarbons by C−H activation is considered to be one of the "holy grails" of modern organometallic and catalytic chemistry.[6]

During the last years we have focused our attention on C−H activation reactions of α,β-unsaturated imines induced by carbonyls of the group 8 metal iron or ruthenium. We developed catalytic reactions in which the C−H activation steps were used to form new carbon−carbon bonds and which by selective reaction cascades allow the synthesis of heterocyclic compounds such as dihydropyrrol-2-one or dihydrobenzoisoindol-2-one derivatives in excellent yields.[7] We also synthesized stable transition metal compounds from the substrates of the catalytic reactions in order to gain some information on the initial steps of the catalytic cycles, especially on the C−H activation step.[8] The reaction of $Fe_2(CO)_9$ with aromatic imines leads to the formation of dinuclear iron carbonyl complexes, in which the ligand reacts via a C−H activation in ortho-position with respect to the exocyclic imine moiety. The abstracted hydrogen atom is transferred to the former imine carbon atom by a formal 1,3-hydrogen shift reaction producing a methylene group. We also observed hydrogen transfer reactions toward the imine nitrogen atom or toward one of the aromatic carbon atoms of the imine.[8] The use of bifunctional imine ligands derived from terephthalic aldehyde resulted in the formation of di-, tri-, or tetranuclear iron carbonyl compounds showing the same reactivity patterns at the central aromatic ring as those observed for benzaldehyde or naphthylaldehyde derivatives.[8]

In this report we wish to describe the synthesis of iron carbonyl complexes from bifunctional imines derived from diamine systems. We also want to show that there is an electronic communication between the two dinuclear subunits of the resulting compounds depending on the nature of the bridging unit especially by measurements of the magnetic susceptibility and the cyclic voltammograms of the complexes.

Synthesis and Characterization. Scheme 1 shows the reaction of the di-imine ligands **1**−**5** with $Fe_2(CO)_9$. **1**−**5** are easily prepared by condensation of 2 equiv of benzaldehyde with the corresponding diamines (see Experimental Part). The imino groups are separated by different bridging units X like phenylene (**1**), biphenylene (**2**), diphenylmethano (**3**), diphenyl ether (**4**), or diphenyl thioether (**5**), respectively. The reaction with

(4) (a) Broadwater, J. A.; Ai, J.; Loehr, T. M.; Sanders-Loehr, J.; Fox, B. G. *Biochemistry* **1998**, *37*, 14664. (b) Subbe, J.; van der Donk, W. A. *Chem. Rev.* **1998**, *98*, 705. (c) Moënne-Loccoz, P.; Baldwin, J.; Lay, B. A.; Loehr, M.; Bollinger, J. J. M. *Biochemistry* **1998**, *37*, 14659. (d) Moënne-Loccoz, P.; Krebs, C.; Herlihy, K.; Edmondson, D. E.; Theil, E. C.; Huynh, B. H.; Loehr, T. M. *Biochemistry* **1999**, *38*, 5290. (e) Hwang, J.; Krebs, C.; Huynh, B. H.; Edmondson, D. E.; Theil, E. C.; Penner-Hahn, J. E. *Science* **2000**, *287*, 122. (f) Solomon, E. I.; Sundaram, U. M.; Machonkin, T. E. *Chem. Rev.* **1996**, *96*, 2563. (g) Sánchez-Ferrer, A.; Rodríguez-López, J. N.; García-Cánovas, F.; García-Carmona, F. *Biochim. Biophys. Acta* **1995**, *1247*, 1. (h) Solomon, E. I.; Chen, P.; Metz, M.; Lee, S.-K.; Palmer, A. E. *Angew. Chem., Int. Ed.* **2001**, *40*, 4570. (i) Que, L., Jr.; Tolman, W. B. *Angew. Chem., Int. Ed.* **2002**, *41*, 1114.

(5) (a) Wallar, B. J.; Lipscomb, J. D. *Chem. Rev.* **1996**, *96*, 2625. (b) Feig, A. L.; Lippard, S. J. *Chem. Rev.* **1994**, *94*, 759. (c) Merkx, M.; Kopp, D. A.; Sazinsky, M. H.; Blaszyk, J. L.; Müller, J.; Lippard, S. J. *Angew. Chem., Int. Ed.* **2001**, *40*, 2782. (d) Brazeau, B. J.; Austin, R. N.; Tarr, C.; Groves, J. T.; Lipscomb, J. D. *J. Am. Chem. Soc.* **2001**, *123*, 11831. (e) Musaev, D. G.; Basch, H.; Morokuma, K. *J. Am. Chem. Soc.* **2002**, *124*, 4135. (f) Liu, Z.-P.; Hu, P.. *J. Am. Chem. Soc.* **2002**, *124*, 5175.

(6) (a) Guari, Y.; Sabo-Etienne, S.; Chaudret, B. *Eur. J. Inorg. Chem.* **1999**, 1047. (b) Dyker, G. *Angew. Chem.* **1999**, *38*, 1698. (c) Bergman, R. G. *Acc. Chem. Res.* **1995**, *28*, 154. (d) Crabtree, R. H. *Chem. Rev.* **1995**, *95*, 987. (e) Zhong, H. A.; Labinger, J. A.; Bercaw, J. E. *J. Am. Chem. Soc.* **2002**, *124*, 1378. (f) Ritleng, V.; Sirlin, C.; Pfeffer, M. *Chem. Rev.* **2002**, *102*, 1731.

(7) (a) Berger, D.; Imhof, W. *J. Chem. Soc., Chem. Commun.* **1999**, 1457. (b) Berger, D.; Imhof, W. *Tetrahedron* **2000**, *56*, 2015. (c) Berger, D.; Göbel, A.; Imhof, W. *J. Mol. Catal A: Chem.* **2001**, *165*, 37. (d) Imhof, W.; Berger, D.; Kötteritzsch, M.; Rost, M.; Schönecker, B. *Adv. Synth. Catal.* **2001**, *343*, 795.

(8) (a) Imhof, W. *J. Chem. Soc., Dalton Trans.* **1996**, 1429. (b) Imhof, W. *J. Organomet. Chem.* **1997**, *533*, 31. (c) Imhof, W. *J. Organomet. Chem.* **1997**, *541*, 109. (d) Imhof, W.; Göbel, A.; Ohlmann, D.; Flemming, J.; Fritzsche, H. *J. Organomet. Chem.* **1999**, *584*, 33. (e) Imhof, W. *Organometallics* **1999**, *18*, 4845. (f) Imhof, W.; Göbel, A. *J. Organomet. Chem.* **2000**, *610*, 102.

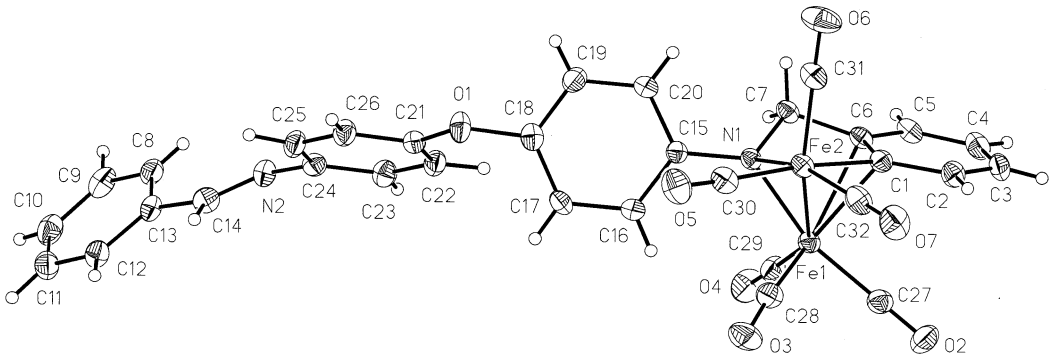

Figure 1. Molecular structure of **14**.

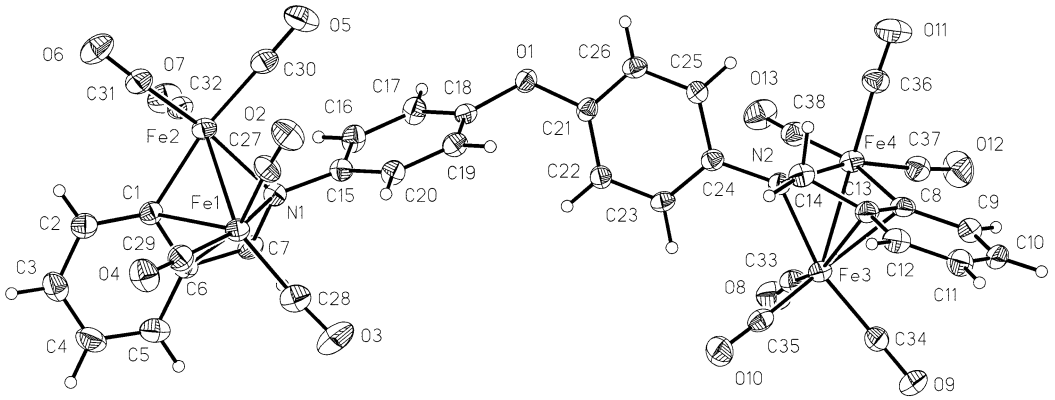

Figure 2. Molecular structure of **9**.

$Fe_2(CO)_9$ yields the di- and tetranuclear iron carbonyl complexes **6**−**15**. It is obvious that the reaction proceeeds via the expected pathway of ortho-metalation with a subsequent 1,3-hydrogen shift reaction either on one or on both sides of the ligand. Chromatographic workup of the crude reaction mixtures yields the less polar tetranuclear compounds **6**−**10** first, followed by the dinuclear derivatives **11**−**15**.

Structure Determinations. By recrystallization of crude **6**, **9**−**11**, **13**, and **14** from mixtures of light petroleum (bp 40−60 °C) and CH_2Cl_2, crystals suitable for X-ray structure determination are obtained. The molecular structures of the complexes **9** and **14** are shown in Figures 1 and 2, and selected bond lengths and angles of all structurally characterized compounds are depicted in Tables 1 and 2.

In all compounds the dinuclear iron carbonyl coordinated subunits are built up in the same way. The corresponding ligand is metalated in ortho position with respect to the exocyclic imine function. The hydrogen atom is transferred to the former imine carbon atom by an intramolecular 1,3-hydrogen shift reaction, producing a methylene group instead. The ligand thus may be described as a six-electron-donating enyl-amido ligand coordinating an $Fe_2(CO)_6$ moiety. Alternatively, the coordination mode could be formulated as an aza-ferra-cyclopentadiene ligand which is facially coordinated by another $Fe(CO)_3$ group.[8]

In **11**, **13**, and **14** (Figure 1) only one of the imine functions is coordinated to the iron carbonyl fragments. The bond lengths and angles in the complex fragment of all three dinuclear compounds are essentially identical (Table 1). The iron−iron bond length is in the range of a single bond. The most interesting fact is that in accordance with the structural analyses of related compounds of a series of aromatic imines the bond lengths between the apical iron atom and the carbon atoms of the aromatic ring (C1, C6) are significantly different.[8] The bond between Fe1 and C1, which formally is a carbanion and shows bonding interactions with both iron atoms, is always about 15 pm shorter than the Fe1−C6 bond. The aromatic ring attached to N1 is nearly perpendicular to the aza-ferra-cyclopentadiene system. It is slightly moved out of an ideal perpendicular arrangement in order to avoid steric interactions with the CO ligands at Fe2. The second imine moiety remains largely unchanged, posessing a carbon−nitrogen double bond length as well as a trans configuration. In **13** and **14** the two central aromatic ring systems attached to the bridging methylene group

Table 1. Selected Bond Lengths [Å] and Angles [deg] of 11, 13, and 14

	11	**13**	**14**
Fe1−Fe2	2.454(2)	2.4456(6)	2.4466(6)
Fe1−C1	2.193(3)	2.180(3)	2.183(3)
Fe1−C6	2.342(3)	2.355(3)	2.335(3)
Fe1−N1	1.990(3)	1.970(2)	1.973(2)
Fe2−C1	2.003(3)	1.997(3)	1.995(3)
C1−C6	1.425(4)	1.419(4)	1.414(4)
C6−C7	1.519(4)	1.496(4)	1.500(4)
C7−N1	1.494(4)	1.482(3)	1.479(4)
Fe2−N1	2.000(2)	1.990(2)	1.992(2)
C14−N2	1.274(4)	1.265(4)	1.260(4)
C1−Fe2−N1	79.2(1)	78.7(1)	78.9(1)
Fe2−C1−C6	113.6(2)	113.5(2)	113.7(2)
C1−C6−C7	114.4(3)	114.0(3)	113.7(2)
C6−C7−N1	101.4(2)	102.1(2)	102.2(2)
C7−N1−Fe2	111.3(2)	110.5(2)	110.5(2)
C7−N1−C15	113.5(2)	113.8(2)	114.4(2)
Fe2−N1−C15	121.9(2)	120.8(2)	120.3(2)
C14−N2−C_{ipso}	118.9(3)	118.6(3)	118.6(3)
N2−C14−C13	122.1(3)	124.3(3)	122.8(3)

Table 2. Selected Bond Lengths [Å] and Angles [deg] of 6, 9, and 10

	6	9	10
Fe1−Fe2	2.4542(7)	2.4642(6)	2.449(2)
Fe1−C1	2.195(3)	2.170(3)	2.19(1)
Fe1−C6	2.382(3)	2.297(3)	2.39(1)
Fe1−N1	1.971(3)	1.976(2)	1.996(9)
Fe2−C1	2.007(3)	1.978(3)	2.02(1)
C1−C6	1.420(5)	1.427(4)	1.42(2)
C6−C7	1.509(5)	1.506(4)	1.52(2)
C7−N1	1.494(4)	1.473(4)	1.49(2)
Fe2−N1	1.982(3)	1.969(3)	1.990(9)
Fe3−Fe4		2.4660(6)	2.433(3)
Fe3−C8		2.170(3)	2.19(1)
Fe3−C13		2.325(3)	2.36(1)
Fe3−N2		1.975(2)	1.97(1)
Fe4−C8		1.994(3)	2.01(1)
C8−C13		1.421(4)	1.39(2)
C13−C14		1.503(4)	1.52(2)
C14−N2		1.483(4)	1.48(2)
Fe4−N2		1.976(3)	1.98(1)
C1−Fe2−N1	78.5(1)	79.2(1)	79.6(4)
Fe2−C1−C6	113.9(2)	113.3(2)	112.8(8)
C1−C6−C7	114.3(3)	114.1(3)	114(1)
C6−C7−N1	101.6(3)	101.0(2)	103.3(9)
C7−N1−Fe2	112.1(2)	112.1(2)	110.8(7)
C7−N1−C_{ipso}	112.5(3)	114.5(3)	113.7(9)
Fe2−N1−C_{ipso}	120.2(2)	118.2(3)	121.2(7)
C8−Fe4−N2		78.8(1)	78.4(5)
Fe4−C8−C13		113.4(2)	113(1)
C8−C13−C14		114.2(3)	116(1)
C13−C14−2		101.5(3)	100.2(9)
C14−N2−Fe4		111.6(6)	112.6(7)
C14−N2−C_{ipso}		114.0(2)	112.9(9)
Fe4−N2− C_{ipso}		119.3(2)	120.4(8)

(**13**) or oxygen atom (**14**), respectively, show torsional angles of about 75°.

In the molecular structure of **6** the center of the bridging phenyl group is a crystallographic center of inversion. Thus the complex shows a trans configuration. The bond lengths and angles between the iron carbonyl fragments and the ligand are nearly identical when compared to the dinuclear compound **11** (Tables 1 and 2). Now the central phenyl ring exhibits a nearly ideal perpendicular arrangement toward the aza-ferra-cyclopentadiene ligands. This is presumably caused by an identical steric pressure from both iron tricarbonyl fragments inside the aza-ferra-cyclopentadiene systems.

The molecular structures of **9** (Figure 2) and **10** are only different in terms of the bridging unit, which exhibits an oxygen atom in **9** and a sulfur atom in **10**. The bond lengths and angles for both compounds show that the two dinuclear subunits are identical (Table 2). In comparison with the molecular structure of **10**, in **9** the iron−iron bond length is slightly longer, whereas the Fe1−C1 and Fe3−C20 bonds are longer compared to the corresponding bond length in **10**. The most significant change is observed in the bond length of Fe1 or Fe3, respectively, to C6 (C25), which is 10 pm longer in **9** when compared to **10**. We showed before that this bond length may be varied over a wide range as a function of the electronic properties of the aromatic system attached to the iron carbonyl moiety. Increasing electron deficiency of the aromatic system results in a longer iron−carbon bond length of the apical iron atom toward the aromatic carbon atom next to the methylene group.[8d] So the electronic differences caused by the presence of an ether or a thioether bridging unit, respectively, obviously has some influence on the bonding in the dinuclear subunits of the tetranuclear complexes.

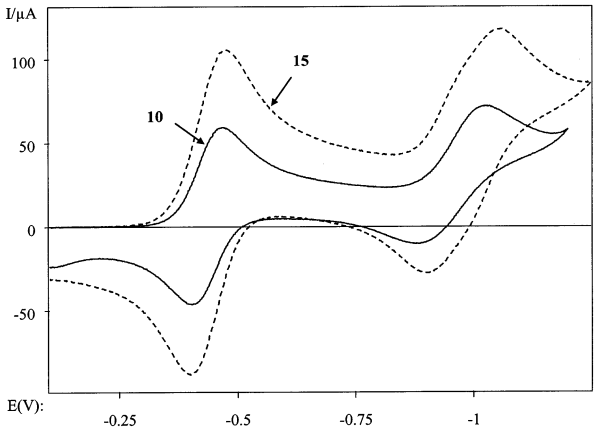

Figure 3. Cyclic voltammograms of **10** and **15**.

When **9** is compared to the dinuclear derivative **14**, it can be seen that the bonding in the complex subunits is identical. The same finding is made for the torsion of the aromatic rings attached to the bridging oxygen atom. In **10** this torsional angle is slightly smaller due to the longer sulfur−carbon bond lengths.

In summary, the molecular structures of **6**, **9**−**11**, **13**, and **14** show properties very similar to those observed for related dinuclear compounds with ligands that contain only one imine moiety. Especially, there is no structural evidence for a communication between the two dinuclear subunits since the bond lengths in **6** and **11** or **9** and **14**, respectively, which are based on the same ligand, do not show any significant changes.

Cyclic Voltammetry. The redox behavior of all iron carbonyl complexes **6**−**15** was studied by means of cyclic voltammetry. Figure 3 shows the cyclic voltammograms of **10** and **15**, which both are synthesized from the same ligand **5**. The dinuclear compounds **11**−**15** all show one reversible reduction wave at about −0.44 V and a second quasi-reversible reduction at about −0.95 V. The cyclic voltammograms of the tetranuclear complexes **6**−**10** show a very similar behavior, but the current intensities are about double when compared to those of **11**−**15**. It has to be pointed out that the uncoordinated ligand shows neither a reduction nor an oxidation wave.

A detailed study of the cyclic voltammograms for the first reduction of the tetranuclear complexes reveals that this process consists of two one-electron reduction steps (Figure 4, Table 3), where the difference between both reduction potentials is usually so small that the charge transfer processes had to be analyzed by fitting the experimental curves to simulated ones. This was accomplished with the aid of the software package DigiSim.[9a,b] The difference between these two reduction steps obtained in this way depends on the nature of the bridging unit, clearly demonstrating that there is a communication between the organometallic moieties on both sides of the ligand. If the bridging unit is a phenyl ring (**6**), the two one-elctron reduction potentials differ by 75 mV. Unfortunately the cyclic voltammogram of **7** could not be simulated due to decomposition reactions

(9) (a) Rudolph, M. In *Physical Chemistry: Principles, Methods and Applications*; Rubinstein, I., Ed.; Marcel Dekker: New York, 1995. (b) Rudolph, M.; Feldberg, S. W. *DigiSim 3.0*; Bioanalytical Systems Inc.: West Lafayette, IN 47906, 1999. (c) Ammar, F.; Saveant, J.-M. *J. Electroanal. Chem.* **1973**, *47*, 215. (d) Flanagan, J. B.; Margel, S.; Bard, A. J.; Anson, F. C. *J. Am. Chem. Soc.* **1978**, *100*, 4248.

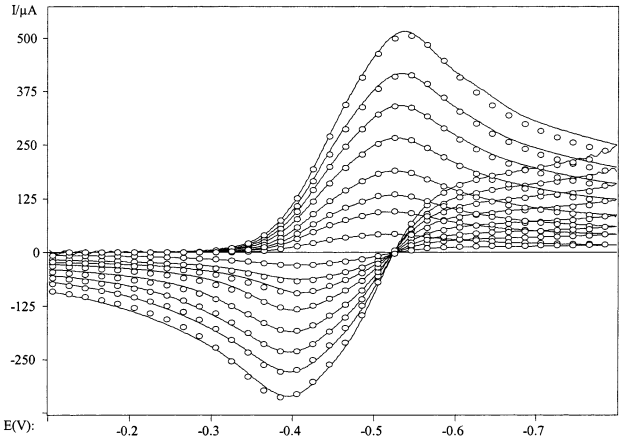

Figure 4. Experimental and calculated cyclic voltammograms of **6** at different scan rates (v = 1, 5, 10, 20, 40, 65, and 100 V/s).

Table 3. Redox Potentials [V] and Rate Constants [cm s^{-1}] of the Charge Transfer Reactions of 6−15

compound	$E_1{}^0$	k_{s1}	E_2	k_{s2}
6	−0.427	0.17	−0.502	0.30
7				
8	−0.436	0.20	−0.477	0.27
9	−0.407	0.20	−0.462	0.17
10	−0.411	0.23	−0.461	0.39
11	−0.448	0.12		
12	−0.442	0.19		
13	−0.447	0.13		
14	−0.449	0.10		
15	−0.436	0.22		

upon reduction of the complex. If the bridging unit exhibits sp^3 hybridized atoms, which formally break up conjugation between the two sides of the ligand system, the difference of the potentials of the first two reduction steps is reduced to 55 mV (**9**), 50 mV (**10**), and 41 mV (**8**), respectively. The last potential difference comes close to the theoretical value of 35.6 mV that will be observed in the limiting case where the electronic interaction between the metal centers tends toward zero.[9c,d] The quasi-reversible reduction waves at about −0.95 V could not be separated into two one-electron steps by digital simulation because the shape of the experimental CVs was affected by chemical reactions induced by the charge transfer process. The nature of these decomposition reactions could not be identified within the framework of the present paper.

Rate constants as well as diffusion coefficients are of expected order of magnitude. So in conclusion it becomes evident by the cyclic voltammograms that in each dinuclear subunit of the iron carbonyl complexes one iron atom is very easily and reversibly reduced, whereas the reduction of the second iron center needs a much higher reduction potential and is not fully reversible. If two dinuclear subunits are present in the molecules, again one iron atom per subunit is reduced at low potentials. These two reduction steps are not observed at the same potential, which is expected to a certain extent since the reduction of a compound already bearing a negative charge is more difficult. Nevertheless, the differences of the potentials we observed are significantly higher. If the bridging unit is fully conjugated, the difference is large due to an effective communication between both sides of the ligand through the bridging unit. In addition, the communication between both dinuclear subunits in **6**−**10** is clearly an intramolecular process since the CV measurements were performed in solution.

Spectroscopic Properties. The results of the electrochemical investigations caused us to determine the oxidation states of the iron atoms especially in the tetranuclear complexes. So compounds **6** and **10** were investigated by means of Mössbauer spectroscopy. Both spectra show essentially the same parameters. Figure 5 displays the Mössbauer spectrum of **10**. It becomes clear that there are two slightly different sets of iron atoms Fe_a and Fe_b. The isomeric shifts are determined at 0.10 mm/s (**10**, quadrupole splitting 1.30 mm/s) and 0.08 mm/s (**6**, quadrupole splitting 1.38 mm/s) for Fe_a and at −0.04 mm/s (**10**, quadrupole splitting 0.87 mm/s) and −0.06 mm/s (**6**, quadrupole splitting 0.85 mm/s) for Fe_b, respectively. These values correspond very well with those reported in the literature for closely related dinuclear iron carbonyl complexes with similar coordination modes of the metal atoms.[10] The isomeric shifts as well as the quadrupole coupling constants are indicative of iron(I) with $S = 1/2$.[10,11] This is consistent with the fact that all tetranuclear complexes might be reduced four times. On the other hand, there are no signifiant differences in the Mössbauer spectra of **6** and **10** even though these compounds show different electrochemical properties (vide infra).

Although the Mössbauer spectra of **6** and **10** suggest the oxidation state +1 for the iron atoms, **6**−**15** show NMR spectroscopic properties as expected for diamagnetic compounds. The chemical shifts in the ^1H and ^{13}C NMR spectra of **6**−**15** are of expected values when compared to similar compounds derived from ligands with only one imine group. The most significant changes in the spectra arise from the fact that one (**11**−**15**) or both (**6**−**10**) imine moieties disappear in the NMR spectra and a signal typical for a methylene group is detected instead. In addition, solid state NMR of **6** and **10** have been aquired in order to investigate whether the spectroscopic properties are different in the solid state. Figure 6 shows a comparison of the ^{13}C NMR spectra of **10** in solution and in the solid state. The solid state NMR spectrum shows signals in the same region as the spectrum recorded in solution. The observed differences result from reduced degrees of freedom in the solid state, which is shown clearly for the resonances of the terminal CO ligands. In solution only one signal is observed since all $Fe(CO)_3$ moieties rotate and interchange at a rate that is fast on the NMR time scale. In the solid state these processes are not possible any more and the CO ligands are no longer indistinguishable. In addition, of course several rotational sidebands are observed in the solid state NMR of **10**.

It is also noteworthy that all iron carbonyl complexes **6**−**15** are EPR-silent in solution as well as in a frozen solution or in measurements using the pure compounds in their solid state (room temperature and 77 K).

(10) Trusov, V. V.; Nekhaev, A. I.; Maksimov, Y. V.; Tyurin, V. D. *Izv. Akad. Nauk. SSSR, Ser. Khim.* **1985**, 1903.

(11) (a) Dilworth, J. R.; Morton, S.; O'Connor, M.; Silver, J. *Inorg. Chim. Acta* **1987**, *127*, 91. (b) Brint, R. P.; O'Cuill, K.; Spalding, T. R.; Deeney, F. A. *J. Organomet. Chem.* **1983**, *247*, 61. (c) Kisch, H.; Krüger, C.; Marcolin, H. E.; Trautwein, A. X. *Z. Naturforsch., B: Chem. Sci.* **1987**, *42*, 1435. (d) Matveev, V. V.; Kolobkov, B. I.; Nekhaev, A. I. *Izv. Akad. Nauk. SSSR, Ser. Chim.* **1987**, 2616.

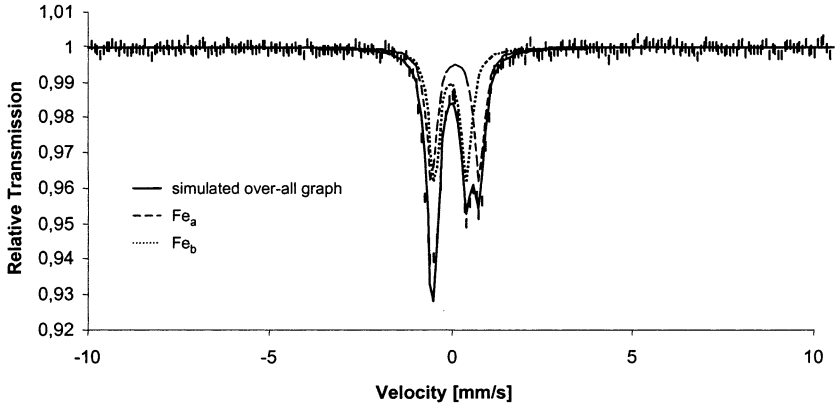

Figure 5. Mössbauer spectrum of **10** indicating two types of iron atoms (Fe_a, Fe_b).

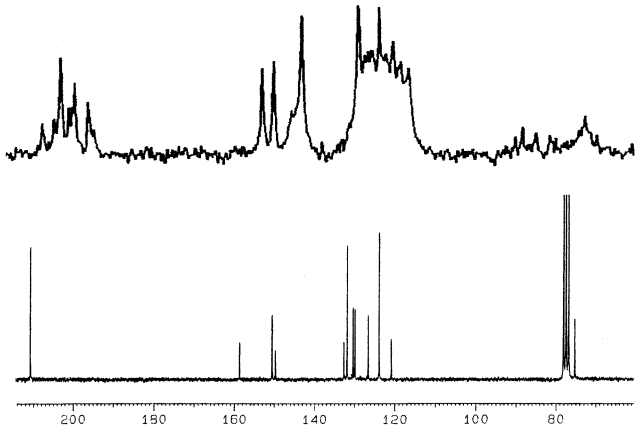

Figure 6. Solid state and solution ^{13}C NMR spectrum of **10**.

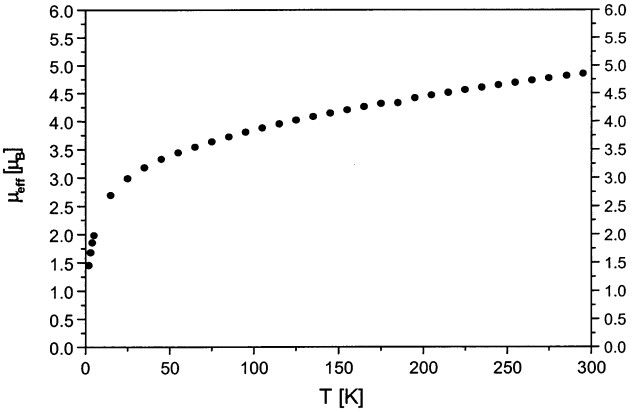

Figure 7. Effective magnetic moment of **8** at variable temperature.

Table 4. Magnetic Moments [μ_B] of 6−15 at Room Temperature

compound	μ_{eff}	compound	μ_{eff}
6	0.71	**11**	0.56
7	1.64	**12**	2.91[a]
8	4.84	**13**	1.37
9	3.56	**14**	1.37
10	3.57	**15**	0.83

[a] Compound **12** was highly affected by chemical reactions following the charge transfer process and decomposed during the measurements as shown by NMR spectroscopy.

Susceptibility Measurements. To gain more insight into the electrochemical properties of the di- and tetranuclear complexes **6**−**15**, we performed susceptibility measurements at variable temperatures. The results are summarized in Table 4. As an example Figure 7 shows the temperature dependency of the effective magnetic moment of **8**.

This plot shows that the effective magnetic moment decreases as the temperature is lowered, pointing to an antiferromagnetic coupling of the Fe(I) centers. The values in Table 4 reveal that all dinuclear complexes **11**−**15** exhibit very low effective magnetic moments. So obviously the spins of the two iron(I) centers in these complexes are effectively coupled by the direct iron−iron bonding. Thus it is not surprising that the behavior of these compounds is that of diamagnetic species in all spectroscopic investigations.

On the other side, it becomes evident that the effective magnetic moment of the tetranuclear iron carbonyl complexes **6**−**10** depends highly on the bridging unit that links the two dinuclear organometallic subunits. The presence of two $Fe_2(CO)_6$ moieties in **6**−**10** leads to effective magnetic moments that cover a wide range. Compound **8**, which exhibits a diphenylmethano bridge between the iron carbonyl moieties, showed the smallest extent of electronic communication in the CV measurements. Correspondingly the effective magnetic moment of **8** amounts to 4.84 μ_B, almost exactly matching the spin-only value of four unpaired electrons all interacting with each other. This would be consistent with the interpretation of the Mössbauer spectra assigning the oxidation state +1 with a low-spin configuration to the iron atoms. As it can be seen from Table 4, the effective magnetic moment decreases the more the bridging unit is capable of establishing electronic communication between both sides of the complex. So the effective magnetic moments of **9** and **10** are nearly identical and slightly smaller than those of **8**. The value for **7** containing a biphenyl bridge is smaller again, as expected, because now the bridging unit consists of sp^2-hybridized atoms only. Compound **6** shows only a small remaining paramagnetism. So obviously in **7** the communication between the iron carbonyl centers is decreased because of the torsion between the phenyl rings in the biphenyl system, whereas the conjugation in **6** is not disturbed at all and so all spins from the iron(I) atoms may be coupled. The fact that all complexes with quite high effective magnetic moment (**8**−**10**) show NMR spectroscopic properties such as diamagnetic compounds may be due to the fact that the spins of four paramagnetic centers (Fe(I) with $S = 1/2$) add to an even

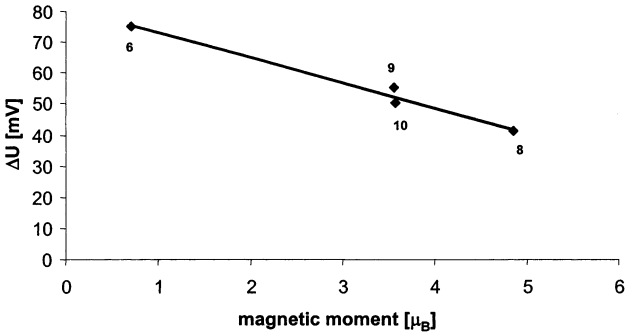

Figure 8. Correlation between electrochemical data and effective magnetic moments of **6** and **8**−**10**.

number of spins, thus producing the macroscopic properties of a diamagnetic compound.

In conclusion it can be stated that there is a nearly linear correlation between the effective magnetic moment and the difference in the potentials representing the reduction of the first iron atom on each side of the tetranuclear complexes. This correlation is shown in Figure 8.

Attempts to reduce one of the tetranuclear compounds **6**−**10** chemically, isolating the corresponding dianion in order to investigate its structure, are ongoing at the moment. We are also planning to do susceptibility measurements at low field. In addition, it is our aim for the future to extend this experimental approach to a number of other bridging units in order to find more evidence for the correlation of CV data and susceptibility measurements for this class of compounds.

Experimental Part

General Procedures. All procedures were carried out under an argon atmosphere in anhydrous, freshly distilled solvents.

Infrared spectra were recorded on a Perkin-Elmer FT-IR System 2000 using 0.2 mm KBr cuvettes. NMR spectra were recorded on a Bruker AC 200 spectrometer (^{1}H, 200 MHz; ^{13}C, 50.32 MHz; $CDCl_3$ as internal standard). Solid state NMR spectra were recorded on a Bruker AMX 400 spectrometer using cross polarization experiments with a sample rotation at the magic angle (CPMAS, ^{1}H, 400.13 MHz; ^{13}C, 100.6 MHz, rotation frequency 12,5 kHz, contact time 6 ms, 293 K). Proton resonances were decoupled (TPPM). EPR spectra were recorded on a Bruker ESP 300 E spectrometer (X-band, 9.4 GHz). Analyses of the spectra were carried out using the program package WinEPR distributed by Bruker.

Susceptibility measurements were obtained on a Quantum-MPMSR-5S-SQUID magnetometer equipped with a 5 T magnet in the range from 2 to 400 K. The samples were contained in a gel bucket and fixed in a nonmagnetic sample holder. Each raw data file for the determination of magnetic moments was corrected for the diamagnetic contribution of the sample holder and the gel bucket. The molar susceptibilities were corrected using the Pascal constant for the metal ions and the increment method according to Haberditzl.[12]

Mass spectra were recorded on a Finnigan MAT SSQ 710 instrument. High-resolution mass spectra were recorded on a Finnigan MAT 95 XL using FAB techniques.

Cyclic voltammetric measurements were conducted with a three-electrode technique using a home-built computer-controlled instrument based on the DAP-3200a data acquisition board (DATALOG Systems). The experiments were performed in methylene chloride containing 0.5 M tetra-*n*-butylammonium-hexafluorophosphate under a blanket of solvent-saturated argon. The ohmic resistance, which had to be compensated for, was determined by measuring the impedance of the system at potentials where the faradaic current was negligibly small. Background correction was accomplished by subtracting the current curves of the blank electrolyte (containing the same concentration of supporting electrolyte) from the experimental CVs. The reference electrode was an Ag/AgCl electrode in acetonitrile containing 0.25 M tetra-*n*-butylammonium chloride. The potential of this reference system was calibrated by measuring the potential of the ferrocenium/ferrocene couple at the end of each experiment. The latter was found to be at 930 mV throughout the measurements. The working electrode was a hanging mercury drop ($m_{Hg-drop}$ = 3.95−4 mg) produced by the CGME instrument (Bioanalytical Systems, Inc.,West Lafayette, IN).

Elemental analyses were carried out at the Institute of Organic and Macromolecular Chemistry at the Friedrich-Schiller-University Jena using a LECO-CHNS-932 system.

X-ray Crystallographic Study. The structure determinations of **6**, **9**, **10**, **11**, **13**, and **14** were carried out on an Enraf Nonius Kappa CCD diffractometer, crystal detector distance 25 mm, 180 frames, using graphite-monochromated Mo Kα radiation. The crystal was mounted in a stream of cold nitrogen. Data were corrected for Lorentz and polarization effects but not for absorption. The structure was solved by direct methods and refined by full-matrix least squares techniques against F^2 using the programs SHELXS86 and SHELXL93.[13] Computation of the structure was acomplished with the program XPMA,[14] and the molecular illustration was drawn using the program XP.[15] The crystal and intensity data are given in Table 5. Additional material on the structure analyses is available from the Cambridge Crystallographic Data Centre by mentioning the deposition number CCDC-194300 (**6**), CCDC-194301 (**9**), CCDC-194302 (**10**), CCDC-194303 (**11**), CCDC-194304 (**13**), or CCDC-194305 (**14**).

Synthesis of 1−**5.** A 0.025 mol sample of the corresponding diamine (2.703 g of 1,4-benzenediamine, 4.606 g of benzidine, 4.954 g of bis(4-aminophenyl)methane, 5.006 g of bis(4-aminophenyl) ether, 5.408 g of bis(4-aminophenyl) thioether) was dissolved in 100 mL of anhydrous ethanol and treated with an excess of benzaldehyde (0.1 mol for the synthesis of **1**, 0.25 mol for the synthesis of **2**, 0.05 mol for the syntheses of **3**−**5**). The solution was stirred at room temperature for 20 h with the exception of the synthesis of **2**, where it was necessary to reflux the solution for 20 h. The precipitate was collected and washed three times with cold ethanol and diethyl ether. Yields: 10.390 g (73.1%) of **1**, 7.164 g (79.5%) of **2**, 7.326 g (78.3%) of **3**, 7.809 g (83.0%) of **4**, 7.939 g (80.9%) of **5**. For a first identification of the compounds their melting points were compared with those reported in the literature.[16]

MS and Spectroscopic Data for 1. MS (CI, H_2O) [*m*/*z*] (fragment, %): 285 (MH^+, 100), 180 ($C_{13}H_{10}N^+$, 8), 152 ($C_{11}H_6N^+$, 8), 142 ($C_{10}H_8N^+$, 14). IR (Nujol, 298 K) [cm^{-1}]: 1616 (s, CH═N). ^{1}H NMR ($CDCl_3$, 298 K) [ppm]: 7.29 (s, 4H, CH_{ar}), 7.48 (s, 6H, CH_{ar}), 7.91 (s, 4H, CH_{ar}), 8.50 (s, 2H, CH═N).[17] ^{13}C NMR ($CDCl_3$, 298 K) [ppm]: 121.9 (CH_{ar}), 128.8 (CH_{ar}), 128.8 (CH_{ar}), 131.3 (CH_{ar}), 136.4 (C_{ar}), 150.1 (C_{ar}), 159.6 (CH═N).

MS and Spectroscopic Data for 2. MS (CI, H_2O) [*m*/*z*] (fragment, %): 361 (MH^+, 100), 273 ($C_{19}H_{17}N_2^+$, 99), 185 ($C_{12}H_{13}N_2^+$, 34), 136 ($C_9H_{14}N^+$, 13), 107 ($C_7H_9N^+$/$C_7H_7O^+$, 3), 65 ($C_5H_5^+$, 24). IR (Nujol, 298 K) [cm^{-1}]: 1639 (s, CH═N). ^{1}H

(12) Haberditzl, W. *Magnetochemie*; Akademie-Verlag, 1968.

(13) (a) Sheldrick, G. *SHELXS-86*; Universität Göttingen, 1986. (b) Sheldrick, G. *SHELXL-93*; Universität Göttingen, 1993.

(14) Zsolnai, L.; Huttner, G. *XPMA*; Universität Heidelberg, 1996.

(15) *XP*−*Interactive Molecular Graphics*, Vers. 4.2; Siemens Analytical X-ray Inst. Inc., 1990.

(16) D'Alelio, G. F.; Crivello, J. V.; Schoenig, R. K.; Huemmer, T. F. *J. Macromol. Sci. Chem.* **1967**, *1*, 1251.

(17) Coville, N. J.; Neuse, E. W. *J. Org. Chem.* **1977**, *42*, 3485.

Table 5. Crystal and Intensity Data for the Compounds 6, 9−11, 13, and 14

	6	9	10	11	13	14
formula	$C_{32}H_{16}N_2O_{12}Fe_4$	$C_{38}H_{20}N_2O_{13}Fe_4$	$C_{38}H_{20}N_2O_{12}SFe_4$	$C_{26}H_{16}N_2O_6Fe_2$	$C_{33}H_{22}N_2O_6Fe_2$	$C_{32}H_{20}N_2O_7Fe_2$
molecular weight [g mol^{-1}]	843.87	935.96	952.02	564.11	654.23	656.20
radiation	Mo Kα	Mo Kα	Mo Kα	Mo Kα	Mo Kα	Mo Kα
monochromator	graphite	graphite	graphite	graphite	graphite	graphite
temperature [K]	183	183	183	183	183	183
cryst color	red	red	red	red	red	red
cryst size [mm]	0.5 × 0.2 × 0.01	0.3 × 0.2 × 0.2	0.4 × 0.3 × 0.2	0.3 × 0.3 × 0.2	0.1 × 0.1 × 0.03	0.2 × 0.1 × 0.1
a [Å]	12.9624(6)	14.5009(8)	8.873(2)	11.0921(7)	8.1792(5)	7.9954(3)
b [Å]	9.6709(4)	15.9608(8)	30.9808(6)	14.857(1)	8.9034(7)	8.8318(4)
c [Å]	14.2766(6)	16.2962(4)	13.734(3)	15.432(1)	20.107(1)	20.1788(8)
α [deg]	90	98.301(3)	90	77.97(5)	95.699(4)	96.05(3)
β [deg]	113.818(2)	94.700(3)	90.61(3)	77.48(6)	95.133(4)	95.16(3)
γ [deg]	90	90.003(2)	90	87.09(6)	95.850(4)	96.93(2)
volume [Å^3]	1637.3(1)	3719.4(3)	3775(1)	2443.8(3)	1422.0(2)	1399.0(1)
Z	2	4	4	4	2	2
F(000)	844	1880	1912	1144	668	668
ρ_{calc} [g cm^{-3}]	1.712	1.671	1.675	1.533	1.507	1.558
cryst syst	monoclinic	triclinic	monoclinic	triclinic	triclinic	triclinic
space group	$P2_1/n$	$P\bar{1}$	$P2_1/n$	$P\bar{1}$	$P\bar{1}$	$P\bar{1}$
abs coeff [mm^{-1}]	1.804	1.599	1.633	1.235	1.058	1.090
θ limit [deg]	$4.16 < \theta < 26.41$	$1.27 < \theta < 27.45$	$1.62 < \theta < 27.49$	$3.32 < \theta < 26.37$	$2.52 < \theta < 27.41$	$2.34 < \theta < 27.45$
scan mode	omega-, phi-scan	omega-, phi-scan	omega-, phi-scan	omega-, phi-scan	omega-, phi-scan	omega-, phi-scan
no. of reflns measd	3340	26 014	4143	9803	10 014	9030
no. of ind reflns	3340	16 553	3098	9803	6443	6125
R_{int}	0.0000	0.0700	0.0229	0.0000	0.0716	0.0307
no. of reflns obsd ($F_o^2 > 2\sigma(F_o^2)$)	2646	7502	2732	7847	3354	4387
no. of params	258	1033	517	777	476	468
goodness-of-fit	1.093	0.624	1.219	1.109	0.845	1.008
R_1	0.0462	0.0368	0.0758	0.0460	0.0437	0.0434
wR_2	0.0788	0.0690	0.1563	0.0908	0.0827	0.0942
final diffraction map electron density peak [e Å^{-3}]	0.428	0.441	0.645	0.419	0.354	0.322

NMR ($CDCl_3$, 298 K) [ppm]: 6.99−7.39 (m, 4H, CH_{ar}), 7.39−7.59 (m, 6H, CH_{ar}), 7.59−7.78 (m, 4H, CH_{ar}), 7.78−8.25 (m, 4H, CH_{ar}), 8.52 (s, 2H, CH=N). ^{13}C NMR ($CDCl_3$, 298 K) [ppm]: 121.4 (CH_{ar}), 127.6 (CH_{ar}), 128.8 (CH_{ar}), 128.8 (CH_{ar}), 131.4 (CH_{ar}), 136.3 (C_{ar}), 138.4 (C_{ar}), 151.2 (C_{ar}), 160.1 (CH=N).

MS and Spectroscopic Data for 3. MS (CI, H_2O) [m/z] (fragment, %): 375 (MH^+, 100), 287 ($C_{20}H_{19}N_2^+$, 5), 270 ($C_{20}H_{16}N^+$, 11), 194 ($C_{14}H_{12}N^+$, 54). IR (Nujol, 298 K) [cm^{-1}]: 1624 (s, CH=N). ^{1}H NMR ($CDCl_3$, 298 K) [ppm]: 4.05 (s, 2H, CH_2), 7.15−7.35 (m, 8H, CH_{ar}), 7.37−7.60 (m, 6H, CH_{ar}), 7.82−7.99 (m, 4H, CH_{ar}), 8.49 (s, 2H, CH=N). ^{13}C NMR ($CDCl_3$, 298 K) [ppm]: 41.0 (CH_2), 121.0 (CH_{ar}), 128.7 (CH_{ar}), 129.6 (CH_{ar}), 131.2 (CH_{ar}), 136.3 (C_{ar}), 139.0 (C_{ar}), 150.2 (C_{ar}), 159.8 (CH=N).

MS and Spectroscopic Data for 4. MS (CI, H_2O) [m/z] (fragment, %)]: 377 (MH^+, 100), 289 ($C_{19}H_{17}N_2O^+$, 24), 196 ($C_{13}H_{10}NO^+$, 28), 107 ($C_7H_9N^+/C_7H_7O^+$, 5). IR (Nujol, 298 K) [cm^{-1}]: 1623 (s, CH=N). ^{1}H NMR ($CDCl_3$, 298 K) [ppm]: 6.98−7.13 (m, 4H, CH_{ar}), 7.15−7.33 (m, 4H, CH_{ar}), 7.37−7.55 (m, 6H, CH_{ar}), 7.80−7.96 (m, 4H, CH_{ar}), 8.48 (s, 2H, CH=N). ^{13}C NMR ($CDCl_3$, 298 K) [ppm]: 119.4 (CH_{ar}), 122.3 (CH_{ar}), 128.7 (CH_{ar}), 131.2 (CH_{ar}), 136.3 (C_{ar}), 147.4 (C_{ar}), 155.8 (C_{ar}), 159.4 (CH=N).

MS and Spectroscopic Data for 5. MS (CI, H_2O) [m/z] (fragment, %)]: 393 (MH^+, 100), 305 ($C_{19}H_{17}N_2S^+$, 51), 212 ($C_{13}H_{10}NS^+$, 19), 182 ($C_{13}H_{12}N^+$, 14), 107 ($C_7H_9N^+/C_7H_7O^+$, 5). IR (Nujol, 298 K) [cm^{-1}]: 1622 (s, CH=N). ^{1}H NMR ($CDCl_3$, 298 K) [ppm]: 7.05−7.21 (m, 4H, CH_{ar}), 7.30−7.42 (m, 4H, CH_{ar}), 7.42−7.60 (m, 6H, CH_{ar}), 7.78−7.97 (m, 4H, CH_{ar}), 8.45 (s, 2H, CH=N). ^{13}C NMR ($CDCl_3$, 298 K) [ppm]: 121.8 (CH_{ar}), 128.8 (CH_{ar}), 128.9 (CH_{ar}), 131.5 (CH_{ar}), 132.0 (CH_{ar}), 133.3 (C_{ar}), 136.2 (C_{ar}), 151.1 (C_{ar}), 160.4 (CH=N).

Synthesis of 6−15. A 500 mg portion of $Fe_2(CO)_9$ (1.37 mmol) together with 0.69 mmol of the corresponding bis-imine ligand (195 mg of **1**, 248 mg of **2**, 257 mg of **3**, 259 mg of **4**, 270 mg of **5**) and 35 mL of *n*-heptane were stirred together at 50−60 °C for 1.5 h. In the course of the reaction the pale yellow suspension slowly turned to a deep red solution as the $Fe_2(CO)_9$ dissolved. After the reaction was complete all volatile materials were removed in vacuo. The residue was dissolved in CH_2Cl_2, 1 g of silanized silica gel was added, and the solvent was again removed under reduced pressure. Chromatography on silica gel using light petroleum (bp 40−60 °C) as the eluent first yielded a small green band containing $Fe_3(CO)_{12}$. Adding small portions of CH_2Cl_2 to the light petroleum allowed the elution of the tetranuclear compounds **6**−**10** followed by the dinuclear complexes **11**−**15**. Compounds **13**, **14**, and **15** were still contaminated with variable portions of the corresponding free ligand. To obtain the pure compounds, they have to be chromatographed again using toluene as the solvent. Recrystallization of the complexes was performed from mixtures of light petroleum (bp 40−60 °C) and CH_2Cl_2 at −20 °C.

MS and Spectroscopic Data for 6. Yield: 37 mg (6.4%). MS (FAB in nitrobenzyl alcohol) [m/z (fragment)]: 844 (M^+), 816 ($M^+ - CO$), 760 ($M^+ - 3CO$), 732 ($M^+ - 4CO$), 704 ($M^+ - 5CO$), 676 ($M^+ - 6CO$), 648 ($M^+ - 7CO$), 620 ($M^+ - 8CO$), 592 ($M^+ - 9CO$), 564 ($M^+ - 10CO$), 536 ($M^+ - 11CO$), 508 ($M^+ - 12CO$), 480 ($M^+ - 11CO - Fe$), 452 ($M^+ - 12CO - Fe$), 424 ($M^+ - 11CO - 2Fe$). HRMS $C_{32}H_{16}N_2O_{12}Fe_4$ (843.87): 843.81303, $C_{32}H_{16}N_2O_{12}Fe_4$ (M^+), $\Delta = -2.9623$ mmu. Anal. Found (calcd): C 45.2 (45.5), H 2.0 (1.9), N 3.2 (3.3). IR (Nujol, 298 K) [cm^{-1}]: 2066 (w) (C=O), 2020 (m) (C=O), 2004 (m) (C=O), 1989 (m) (C=O), 1975 (m) (C=O), 1931 (w) (C=O). ^{1}H NMR ($CDCl_3$, 298 K) [ppm]: 4.30 (s, 4H, CH_2−N), 6.88 (s, 4H, CH_{ar}), 7.07 (dd, $^3J_{HH}$ = 7.1 Hz, $^3J_{HH}$ = 7.1 Hz, 2H, CH_{ar}), 7.29 (dd, $^3J_{HH}$ = 7.2 Hz, $^3J_{HH}$ = 7.2 Hz, 2H, CH_{ar}), 7.57 (d, $^3J_{HH}$ = 7.9 Hz, 2H, CH_{ar}), 8.00 (d, $^3J_{HH}$ = 8.0 Hz, 2H, CH_{ar}). ^{13}C NMR ($CDCl_3$, 298 K) [ppm]: 75.0 (CH_2−N), 120.6 (C_{ar}), 123.0 (CH_{ar}),

126.1 (CH_{ar}), 129.4 (CH_{ar}), 129.9 (CH_{ar}), 149.1 (C_{ar}), 150.1 (CH_{ar}), 156.1 (C−Fe), 210.3 (CO). Solid state NMR (293 K): 76.6 (CH_2−N), 121.6 (CH_{ar}), 123.3 (C_{ar}), 126.5 (CH_{ar}), 127.7 (CH_{ar}), 129.8 (CH_{ar}), 131.8 (CH_{ar}), 148.2 (C_{ar}), 150.3 (CH_{ar}), 157.4 (C−Fe), 206.2 (CO), 209.7 (CO), 211.9 (CO), 212.9 (CO), 218.7 (CO). Mössbauer spectrum (77 K): 2 doublets; fit, $\sigma = -0.06$ mm s^{-1}, $\Delta E_Q = 0.85$ mm s^{-1}, $\sigma = 0.08$ mm s^{-1}, $\Delta E_Q = 1.38$ mm s^{-1}. Susceptibility measurement (295 K): $\mu_{eff} = 0.71\ \mu_B$.

MS and Spectroscopic Data for 11. Yield: 115 mg (29.7%). MS (FAB in nitrobenzyl alcohol) [*m*/*z* (fragment)]: 565 (MH^+), 537 ($MH^+ - CO$), 508 ($M^+ - 2CO$), 480 ($M^+ - 3CO$), 452 ($M^+ - 4CO$), 424 ($M^+ - 5CO$), 396 ($M^+ - 6CO$), 340 ($M^+ - 6CO - Fe$), 283 ($C_{20}H_{15}N_2^+$). HRMS $C_{26}H_{16}N_2O_6Fe_2$ (564.12): 564.98115, $C_{26}H_{17}N_2O_6Fe_2$ (MH^+), $\Delta = -2.6169$ mmu. Anal. Found (calcd): C 55.5 (55.3), H 2.9 (2.8), N 5.2 (4.9). IR (Nujol, 298 K) [cm^{-1}]: 2064 (s) (C═O), 2028 (vs) (C═O), 1996 (vs) (C═O), 1986 (vs) (C═O), 1976 (sh, vs) (C═O), 1962 (vs) (C═O), 1925 (s) (C═O), 1629 (m) (C═N). ^{1}H NMR ($CDCl_3$, 298 K) [ppm]: 4.37 (s, 2H, CH_2−N), 7.07 (s, 4H, CH_{ar}), 7.08 (dd, $^3J_{HH} = 7.2$ Hz,$^3J_{HH} = 7.2$ Hz, 1H, CH_{ar}), 7.31 (dd, $^3J_{HH} = 7.2$ Hz,$^3J_{HH} = 7.2$ Hz, 1H, CH_{ar}), 7.38−7.55 (m, 3H, CH_{ar}), 7.59 (d, $^3J_{HH} = 7.9$ Hz, 1H, CH_{ar}), 7.79−7.96 (m, 2H, CH_{ar}), 8.02 (d, $^3J_{HH} = 8.1$ Hz, 1H, CH_{ar}), 8.43 (s, 1H, CH═N). ^{13}C NMR ($CDCl_3$, 298 K) [ppm]: 75.2 (CH_2−N), 120.6 (C_{ar}), 121.3 (CH_{ar}), 123.4 (CH_{ar}), 126.0 (CH_{ar}), 128.8 (CH_{ar}), 129.3 (CH_{ar}), 129.9 (CH_{ar}), 131.4 (CH_{ar}), 136.2 (C_{ar}), 149.1 (C_{ar}), 149.2 (C_{ar}), 150.1 (CH_{ar}), 157.1 (C−Fe), 160.1 (CH═N), 210.4 (CO). Susceptibility measurement (295 K): $\mu_{eff} = 0.56\ \mu_B$.

MS and Spectroscopic Data for 7. Yield: 127 mg (20.1%). MS (FAB in nitrobenzyl alcohol) [*m*/*z* (fragment)]: 920 (M^+), 892 ($M^+ - CO$), 865 ($MH^+ - 2CO$), 836 ($M^+ - 3CO$), 808 ($M^+ - 4CO$), 780 ($M^+ - 5CO$), 752 ($M^+ - 6CO$), 724 ($M^+ - 7CO$), 696 ($M^+ - 8CO$), 668 ($M^+ - 9CO$), 640 ($M^+ - 10CO$), 613 ($MH^+ - 11CO$), 584 ($M^+ - 12CO$), 555 ($M^+ - 11CO - Fe - H$), 527 ($M^+ - 12CO - Fe - H$), 499 ($M^+ - 11CO - 2Fe - H$), 471 ($M^+ - 12CO - 2Fe - H$), 415 ($M^+ - 12CO - 3Fe - H$), 361 ($C_{26}H_{21}N_2^+$), 359 ($C_{26}H_{19}N_2^+$). HRMS $C_{38}H_{20}N_2O_{12}Fe_4$ (919.97): 919.84786, $C_{38}H_{20}N_2O_{12}Fe_4$ (M^+), $\Delta = -6.4922$ mmu. IR (Nujol, 298 K) [cm^{-1}]: 2061 (s) (C═O), 2050 (m) (C═O), 2019 (s) (C═O), 2005 (s) (C═O), 1975 (s, br) (C═O), 1939 (s, br) (C═O). ^{1}H NMR ($CDCl_3$, 298 K) [ppm]: 4.38 (s, 4H, CH_2−N), 7.00−7.17 (m, 6H, CH_{ar}), 7.31 (dd, $^3J_{HH} = 7.4$ Hz, $^3J_{HH} = 7.4$ Hz, 2H, CH_{ar}), 7.37−7.51 (m, 4H, CH_{ar}), 7.60 (d,$^3J_{HH} = 7.7$ Hz, 2H, CH_{ar}), 8.02 (d, $^3J_{HH} = 8.2$ Hz, 2H, CH_{ar}). ^{13}C NMR ($CDCl_3$, 298 K) [ppm]: 75.0 (CH_2−N), 120.4 (C_{ar}), 123.0 (CH_{ar}), 126.1 (CH_{ar}), 127.1 (CH_{ar}), 129.5 (CH_{ar}), 129.9 (CH_{ar}), 137.0 (C_{ar}), 149.3 (C_{ar}), 150.1 (CH_{ar}), 158.3 (C−Fe), 210.4 (CO). Susceptibility measurement (295 K): $\mu_{eff} = 1.64\ \mu_B$.

MS and Spectroscopic Data for 12. Yield: 43 mg (9.8%). MS (FAB in nitrobenzyl alcohol) [*m*/*z* (fragment)]: 641 (MH^+), 613 ($MH^+ - CO$), 584 ($M^+ - 2CO$), 556 ($M^+ - 3CO$), 528 ($M^+ - 4CO$), 500 ($M^+ - 5CO$), 472 ($M^+ - 6CO$), 415 ($M^+ - 6CO - Fe - H$), 361 ($C_{26}H_{21}N_2^+$), 359 ($C_{26}H_{19}N_2^+$); HRMS $C_{32}H_{20}N_2O_6Fe_2$ (640.21): 641.00717, $C_{32}H_{21}N_2O_6Fe_2$ (MH^+), $\Delta = 2.66323$ mmu. IR (Nujol, 298 K) [cm^{-1}]: 2063 (s) (C═O), 2026 (vs) (C═O), 2003 (vs) (C═O), 1985 (sh, vs) (C═O), 1975 (vs) (C═O), 1966 (vs) (C═O), 1942 (s) (C═O), 1626 (w) (C═N). ^{1}H NMR ($CDCl_3$, 298 K) [ppm]: 4.40 (s, 2H, CH_2−N), 6.83−7.79 (m, 14H, CH_{ar}), 7.79−7.97 (m, 2H, CH_{ar}), 8.03 (d, $^3J_{HH} = 8.2$ Hz, 1H, CH_{ar}), 8.50 (s, 1H, CH═N). ^{13}C NMR ($CDCl_3$, 298 K) [ppm]: 75.0 (CH_2−N), 120.4 (C_{ar}), 121.4 (CH_{ar}), 123.0 (CH_{ar}), 126.1 (CH_{ar}), 127.2 (CH_{ar}), 127.6 (CH_{ar}), 128.8 (CH_{ar}), 128.9 (CH_{ar}), 129.4 (CH_{ar}), 129.8 (CH_{ar}), 131.4 (CH_{ar}), 136.3 (C_{ar}), 137.6 (C_{ar}), 137.7 (C_{ar}), 149.3 (C_{ar}), 150.1 (CH_{ar}), 151.3 (C_{ar}), 158.2 (C−Fe), 160.2 (CH═N), 210.4 (CO). Susceptibility measurement (295 K): $\mu_{eff} = 2.91\ \mu_B$.

MS and Spectroscopic Data for 8. Yield: 67 mg (10.4%). MS (FAB in nitrobenzyl alcohol) [*m*/*z* (fragment)]: 934 (M^+), 850 ($M^+ - 3CO$), 822 ($M^+ - 4CO$), 794 ($M^+ - 5CO$), 766 ($M^+ - 6CO$), 738 ($M^+ - 7CO$), 710 ($M^+ - 8CO$), 682 ($M^+ - 9CO$), 654 ($M^+ - 10CO$), 626 ($M^+ - 11CO$), 598 ($M^+ - 12CO$), 570 ($M^+ - 11CO - Fe$), 542 ($M^+ - 12CO - Fe$), 514 ($M^+ - 11CO - 2Fe$). HRMS $C_{39}H_{22}N_2O_{12}Fe_4$ (934.00): 933.85393, $C_{39}H_{22}N_2O_{12}Fe_4$ (M^+), $\Delta = 3.08787$ mmu. Anal. Found (calcd): C 49.9 (50.1), H 2.8 (2.4), N 2.8 (3.0). IR (Nujol, 298 K) [cm^{-1}]: 2066 (s) (C═O), 2039 (s) (C═O), 2028 (s) (C═O), 2000 (s) (C═O), 1994 (s) (C═O), 1975 (s) (C═O), 1966 (s) (C═O), 1942 (s) (C═O). ^{1}H NMR ($CDCl_3$, 298 K) [ppm]: 3.86 (s, 2H, CH_2), 4.34 (s, 4H, CH_2−N), 6.97 (s, 8H, CH_{ar}), 7.07 (dd, $^3J_{HH} = 6.9$ Hz, $^3J_{HH} = 6.9$ Hz, 2H, CH_{ar}), 7.29 (dd, $^3J_{HH} = 6.9$ Hz, $^3J_{HH} = 6.9$ Hz, 2H, CH_{ar}), 7.57 (d,$^3J_{HH} = 7.6$ Hz, 2H, CH_{ar}), 8.01 (d, $^3J_{HH} = 7.8$ Hz, 2H, CH_{ar}). ^{13}C NMR ($CDCl_3$, 298 K) [ppm]: 40.4 (CH_2), 75.2 (CH_2−N), 120.6 (C_{ar}), 122.8 (CH_{ar}), 126.0 (CH_{ar}), 129.3 (CH_{ar}), 129.3 (CH_{ar}), 129.8 (CH_{ar}), 137.9 (C_{ar}), 149.4 (C_{ar}), 150.1 (CH_{ar}), 157.1 (C−Fe), 210.4 (CO). Susceptibility measurement (295 K): $\mu_{eff} = 4.84\ \mu_B$.

MS and Spectroscopic Data for 13. Yield: 120 mg (26.7%). MS (FAB in nitrobenzyl alcohol) [*m*/*z* (fragment)]: 655 (MH^+), 627 ($MH^+ - CO$), 598 ($M^+ - 2CO$), 570 ($M^+ - 3CO$), 542 ($M^+ - 4CO$), 514 ($M^+ - 5CO$), 486 ($M^+ - 6CO$), 429 ($M^+ - 6CO - Fe - H$), 373 ($C_{27}H_{21}N_2^+$). HRMS $C_{33}H_{22}N_2O_6Fe_2$ (654.24): 655.0241, $C_{33}H_{23}N_2O_6Fe_2$ (MH^+), $\Delta = 1.38329$ mmu. Anal. Found (calcd): C 59.7 (60.0), H 3.6 (4.1), N 4.2 (4.3). IR (Nujol, 298 K) [cm^{-1}]: 2066 (m) (C═O), 2027 (m) (C═O), 2006 (m) (C═O), 1993 (m) (C═O), 1983 (m) (C═O), 1975 (m) (C═O), 1941 (w) (C═O), 1624 (vw) (C═N). ^{1}H NMR ($CDCl_3$, 298 K) [ppm]: 3.94 (s, 2H, CH_2), 4.34 (s, 2H, CH_2−N), 6.81−7.25 (m, 9H, CH_{ar}), 7.29 (dd,$^3J_{HH} = 7.3$ Hz, $^3J_{HH} = 7.3$ Hz, 1H, CH_{ar}), 7.38−7.53 (m, 3H, CH_{ar}), 7.57 (d,$^3J_{HH} = 8.0$ Hz, 1H, CH_{ar}), 7.80−7.96 (m, 2H, CH_{ar}), 8.02 (d, $^3J_{HH} = 8.1$ Hz, 1H, CH_{ar}), 8.46 (s, 1H, CH═N). ^{13}C NMR ($CDCl_3$, 298 K) [ppm]: 40.7 (CH_2), 75.2 (CH_2−N), 120.6 (C_{ar}), 121.1 (CH_{ar}), 122.7 (CH_{ar}), 126.0 (CH_{ar}), 128.7 (CH_{ar}), 128.8 (CH_{ar}), 129.3 (CH_{ar}), 129.3 (CH_{ar}), 129.6 (CH_{ar}), 129.8 (CH_{ar}), 131.2 (CH_{ar}), 136.4 (C_{ar}), 138.3 (C_{ar}), 138.6 (C_{ar}), 149.4 (C_{ar}), 150.1 (CH_{ar}), 150.3 (C_{ar}), 157.0 (C−Fe), 159.9 (CH═N), 210.4 (CO). Susceptibility measurement (295 K): $\mu_{eff} = 1.37\ \mu_B$.

MS and Spectroscopic Data for 9. Yield: 98 mg (15.2%). MS (FAB in nitrobenzyl alcohol) [*m*/*z* (fragment)]: 936 (M^+), 908 ($M^+ - CO$), 880 ($M^+ - 2CO$), 852 ($M^+ - 3CO$), 824 ($M^+ - 4CO$), 796 ($M^+ - 5CO$), 768 ($M^+ - 6CO$), 740 ($M^+ - 7CO$), 712 ($M^+ - 8CO$), 684 ($M^+ - 9CO$), 656 ($M^+ - 10CO$), 628 ($M^+ - 11CO$), 600 ($M^+ - 12CO$). HRMS $C_{38}H_{20}N_2O_{13}Fe_4$ (935.97): 935.83982, $C_{38}H_{20}N_2O_{13}Fe_4$ (M^+), $\Delta = -3.5376$ mmu. Anal. Found (calcd): C 48.5 (48.7), H 2.3 (2.1), N 2.9 (3.0). IR (Nujol, 298 K) [cm^{-1}]: 2065 (vs) (C═O), 2034 (vs, br) (C═O), 2012 (sh, vs) (C═O), 2008 (vs) (C═O), 1976 (vs, br) (C═O), 1943 (vs) (C═O). ^{1}H NMR ($CDCl_3$, 298 K) [ppm]: 4.34 (s, 4H, CH_2−N), 6.52−7.19 (m, 8H, CH_{ar}), 7.08 (dd, $^3J_{HH} = 7.4$ Hz, $^3J_{HH} = 7.4$ Hz, 2H, CH_{ar}), 7.30 (dd, $^3J_{HH} = 7.4$ Hz, $^3J_{HH} = 7.4$ Hz, 2H, CH_{ar}), 7.58 (d,$^3J_{HH} = 8.0$ Hz, 2H, CH_{ar}), 8.02 (d, $^3J_{HH} = 8.2$ Hz, 2H, CH_{ar}). ^{13}C NMR ($CDCl_3$, 298 K) [ppm]: 75.6 (CH_2−N), 118.8 (CH_{ar}), 120.7 (C_{ar}), 124.1 (CH_{ar}), 126.1 (CH_{ar}), 129.3 (CH_{ar}), 130.0 (CH_{ar}), 149.2 (C_{ar}), 150.2 (CH_{ar}), 154.2 (C−Fe), 154.5 (C_{ar}), 210.3 (CO). Susceptibility measurement (295 K): $\mu_{eff} = 3.56\ \mu_B$.

MS and Spectroscopic Data for 14. Yield: 132 mg (29.3%). MS (FAB in nitrobenzyl alcohol) [*m*/*z* (fragment)]: 657 (MH^+), 629 ($MH^+ - CO$), 600 ($M^+ - 2CO$), 572 ($M^+ - 3CO$), 544 ($M^+ - 4CO$), 516 ($M^+ - 5CO$), 488 ($M^+ - 6CO$), 461 ($MH^+ - 5CO - Fe$), 377 ($C_{26}H_{21}N_2O^+$). HRMS $C_{32}H_{20}N_2O_7Fe_2$ (656.21): 657.00637, $C_{32}H_{21}N_2O_7Fe_2$ (MH^+), $\Delta = -1.6222$ mmu. Anal. Found (calcd): C 58.7 (58.5), H 3.3 (3.0), N 4.1 (4.3). IR (Nujol, 298 K) [cm^{-1}]: 2068 (s) (C═O), 2019 (s) (C═O), 2005 (s) (C═O), 1987 (s) (C═O), 1972 (s) (C═O), 1941 (s) (C═O), 1622 (w) (CH═N). ^{1}H NMR ($CDCl_3$, 298 K) [ppm]: 4.39 (s, 2H, CH_2−N), 6.75−7.43 (m, 9H, CH_{ar}), 7.35 (dd, $^3J_{HH} = 7.4$ Hz, $^3J_{HH} = 7.4$ Hz, 1H, CH_{ar}), 7.43−7.57 (m, 3H, CH_{ar}), 7.62 (d,$^3J_{HH} = 7.9$ Hz, 1H, CH_{ar}), 7.81−8.01 (m, 2H, CH_{ar}), 8.06 (d, $^3J_{HH} = 8.1$ Hz, 1H, CH_{ar}), 8.50 (s, 1H, CH═N). ^{13}C NMR ($CDCl_3$, 298 K) [ppm]: 75.6 (CH_2−N), 118.7 (CH_{ar}), 119.6

(CH_{ar}), 120.7 (C_{ar}), 122.3 (CH_{ar}), 124.0 (CH_{ar}), 126.1 (CH_{ar}), 128.8 (CH_{ar}), 129.3 (CH_{ar}), 129.9 (CH_{ar}), 131.3 (CH_{ar}), 136.3 (C_{ar}), 147.6 (C_{ar}), 149.2 (C_{ar}), 150.1 (CH_{ar}), 154.3 (C−Fe), 154.6 (C_{ar}), 155.4 (C_{ar}), 159.6 (CH═N), 210.3 (CO). Susceptibility measurement (295 K): $\mu_{eff} = 1.37\ \mu_B$.

MS and Spectroscopic Data for 10. Yield: 45 mg (6.9%). MS (FAB in nitrobenzyl alcohol) [*m*/*z* (fragment)]: 952 (M^+), 925 ($MH^+ - CO$), 896 ($M^+ - 2CO$), 868 ($M^+ - 3CO$), 840 ($M^+ - 4CO$), 812 ($M^+ - 5CO$), 784 ($M^+ - 6CO$), 756 ($M^+ - 7CO$), 728 ($M^+ - 8CO$), 700 ($M^+ - 9CO$), 672 ($M^+ - 10CO$), 644 ($M^+ - 11CO$), 616 ($M^+ - 12CO$). HRMS $C_{38}H_{20}N_2O_{12}SFe_4$ (952.04): 951.81363, $C_{38}H_{20}N_2O_{12}SFe_4$ (M^+), $\Delta = -0.18949$ mmu. IR (Nujol, 298 K) [cm^{-1}]: 2067 (m) (C═O), 2038 (sh, m) (C═O), 2028 (m) (C═O), 2005 (m) (C═O), 1995 (m) (C═O), 1985 (m) (C═O), 1964 (m) (C═O), 1948 (sh, m) (C═O), 1929 (m) (C═O). ^{1}H NMR ($CDCl_3$, 298 K) [ppm]: 4.34 (s, 4H, CH_2−N), 6.82−7.19 (m, 8H, CH_{ar}), 7.08 (dd, $^3J_{HH} = 7.1$ Hz, $^3J_{HH} = 7.1$ Hz, 2H, CH_{ar}), 7.30 (dd, $^3J_{HH} = 7.1$ Hz, $^3J_{HH} = 7.1$ Hz, 2H, CH_{ar}), 7.58 (d,$^3J_{HH} = 8.0$ Hz, 2H, CH_{ar}), 8.00 (d, $^3J_{HH} = 8.1$ Hz, 2H, CH_{ar}). ^{13}C NMR ($CDCl_3$, 298 K) [ppm]: 74.8 (CH_2−N), 120.4 (C_{ar}), 123.4 (CH_{ar}), 126.1 (CH_{ar}), 129.4 (CH_{ar}), 129.9 (CH_{ar}), 131.4 (CH_{ar}), 132.2 (C_{ar}), 149.2 (C_{ar}), 150.1 (CH_{ar}), 158.2 (C−Fe), 210.3 (CO). Solid state NMR (293 K): 72.5 (CH_2−N), 120.5 (C_{ar}/CH_{ar}), 122.5 (C_{ar}/CH_{ar}), 124.6 (C_{ar}/CH_{ar}), 126.6 (C_{ar}/CH_{ar}), 128.4 (C_{ar}/CH_{ar}), 130.3 (C_{ar}/CH_{ar}), 131.5 (C_{ar}/CH_{ar}), 132.3 (C_{ar}/CH_{ar}), 134.1 (C_{ar}/CH_{ar}), 149.2 (CH_{ar}), 151.9 (C_{ar}), 156.8 (C−Fe), 159.9 (C−Fe), 204.8 (CO), 205.9 (CO), 206.4 (CO), 209.9 (CO), 210.5 (CO), 211.5 (CO), 213.7 (CO), 215.6 (CO), 218.9 (CO). Mössbauer spectrum (77 K): 2 doublets; fit, $\sigma = -0.04$ mm s^{-1}, $\Delta E_Q = 0.87$ mm s^{-1}, $\sigma = 0.10$ mm s^{-1}, $\Delta E_Q = 1.30$ mm s^{-1}. Susceptibility measurement (295 K): $\mu_{eff} = 3.57\ \mu_B$.

MS and Spectroscopic Data for 15. Yield: 99 mg (21.4%). MS (FAB in nitrobenzyl alcohol) [*m*/*z* (fragment)]: 673 (MH^+), 645 ($MH^+ - CO$), 616 ($M^+ - 2CO$), 588 ($M^+ - 3CO$), 560 ($M^+ - 4CO$), 532 ($M^+ - 5CO$), 504 ($M^+ - 6CO$), 393 ($C_{26}H_{21}N_2S^+$). HRMS $C_{32}H_{20}N_2O_6SFe_2$ (672.28): 671.97579, $C_{32}H_{20}N_2O_6SFe_2$ (M^+), $\Delta = -1.7091$ mmu. IR (Nujol, 298 K) [cm^{-1}]: 2066 (m) (C═O), 2028 (s) (C═O), 1993 (s) (C═O), 1984 (s, br) (C═O), 1619 (vw) (CH═N). ^{1}H NMR ($CDCl_3$, 298 K) [ppm]: 4.33 (s, 2H, CH_2−N), 6.81−7.41 (m, 10H, CH_{ar}), 7.41−7.54 (m, 3H, CH_{ar}), 7.58 (d,$^3J_{HH} = 7.9$ Hz, 1H, CH_{ar}), 7.79−7.94 (m, 2H, CH_{ar}), 8.00 (d,$^3J_{HH} = 8.2$ Hz, 1H, CH_{ar}), 8.44 (s, 1H, CH═N). ^{13}C NMR ($CDCl_3$, 298 K) [ppm]: 74.9 (CH_2−N), 120.4 (C_{ar}), 121.9 (CH_{ar}), 123.4 (CH_{ar}), 126.1 (CH_{ar}), 128.8 (CH_{ar}), 128.9 (CH_{ar}), 129.4 (CH_{ar}), 129.9 (CH_{ar}), 131.0 (CH_{ar}), 131.5 (CH_{ar}), 132.4 (C_{ar}, CH_{ar}), 133.1 (C_{ar}), 136.2 (C_{ar}), 149.3 (C_{ar}), 150.1 (CH_{ar}), 151.4 (C_{ar}), 157.9 (C−Fe), 160.5 (CH═N), 210.3 (CO). Susceptibility measurement (295 K): $\mu_{eff} = 0.83\ \mu_B$.

Acknowledgment. The authors gratefully acknowledge financial support by the Deutsche Forschungsgemeinschaft (Collaborative Research Center "Metal Mediated Reactions Modeled after Nature", SFB 436). We would also like to thank Dr. P. Hartmann, Institute for Optics and Quantum Optics, Friedrich-Schiller-University, Jena, for the solid state NMR measurements, Dr. V. Schünemann, Dipl.-Phys. P. Wegner, University of Lübeck, and Dipl.-Chem. B. Weber, Friedrich-Schiller-University Jena, for the measurement of Mössbauer spectra.

Supporting Information Available: A listing of the crystallographic data of **6**, **9**, **10**, **11**, **13**, and **14** together with an ORTEP plot of the molecular structures and a packing diagram for each structurally characterized compound. In addition, ^{13}C NMR spectra of **6**−**15** are supplied. This material is available free of charge via the Internet at http://pubs.acs.org.

OM020850I